Integration of Remote Sensing and Aerogeophysical Data Applied in the Geological Characterization of the Ipueira-Medrado Segment, Andorinhas/BA

Integração de Dados de Sensoriamento Remoto e Aerogeofísicos Aplicados na Caracterização Geológica do Segmento Ipueira-Medrado, Andorinhas/BA

Iago Silva Rebouças[1] ⓘ, Sérgio Roberto Bacelar Hühn[1] ⓘ, Mateus de Paula Miranda[2] ⓘ, Ana Rita Gonçalves Neves Lopes Salgueiro[1] ⓘ, Kleiton Camilo da Paz Sales[3] ⓘ & Cynthia Romariz Duarte[1] ⓘ

[1]Universidade Federal do Ceará, Departamento de Geologia, Fortaleza, CE, Brasil
[2]Universidade Estadual de Campinas, Departamento de Geologia, Campinas, SP, Brasil
[3]Companhia de Ferro Ligas da Bahia, Pojuca, BA, Brasil

E-mails: iago.reboucas@hotmail.com; sergio.bacelar@ufc.br; mateuspmiranda@gmail.com; ritasalgueiro@ufc.br; kleiton@ferbasa.com; cynthia.duarte@ufc.br
Corresponding author: Iago Silva Rebouças; iago.reboucas@hotmail.com

Abstract

The segment of the Ipueira-Medrado mines constitutes two of the main chromium mines explored by the Companhia Ferro-ligas da Bahia (Ferbasa) being considered as the main chromium mineralization in the national context. The research area is located in the municipality of Andorinhas, in the north center of the state of Bahia, in the region of Piemonte Norte do Itapicuru. Therefore, the main objective of this work is to use remote sensing and aerogeophysical data to elaborate a geological map of the Ipueira-Medrado mines and to identify new areas for mineral exploration. The Digital Image Processing (PDI) stage was carried out in an environment in the ENVI® 5.3 software for the scenes of the optical Alos and radar images, Palsar. The treatment of magnetic and radiometric data was carried out in the environment of the software Oasis Montaj 9.10 by Geosoft®. In the Geographic Information System (GIS) platform of ArcGis 10.7.1®, multisource data was integrated. This integration supported the protection of local lithology information and the identification of four lithological units: Sienito Itiúba, Santa Luz Unit, São Bento Unit and Vale do Jacurici Complex. In this last unit, a combined analysis between Map Algebra and Fuzzy logic was applied among all input raster data, in order to mark out a zoning of potential areas for the occurrence of mafic-ultramafic rocks. Thus, a good relationship was noted between the results and surface geological models presented in the literature. In view of this, the application of these methods brought an integrated analysis of multisource data for the elaboration of a geological map of the mafic-ultramafic rocks and their fittings in the Ipueira-Medrado segment in the state of Bahia.

Keywords: Geoprocessing; Jacurici Valley; Chromite

Resumo

O segmento das minas Ipueira-Medrado constitui-se como duas das principais minas de cromo explorado pela Companhia Ferro-ligas da Bahia (Ferbasa) sendo considerada como as principais mineralização de cromo em contexto nacional. A área de pesquisa está localizada no município de Andorinhas, no centro norte do estado da Bahia, na região Piemonte Norte Do Itapicuru. Portanto, o principal objetivo deste estudo é utilizar dados de sensoriamento remoto e aerogeofísicos para criar um mapa geológico das minas Ipueira-Medrado e identificar novas áreas para exploração mineral. A etapa de Processamento Digital de Imagem (PDI) foi realizada em ambiente no *software* ENVI® 5.3 para as cenas das imagens óticas Alos e de radar, Palsar. O tratamento dos dados magnéticos e radiométricos foram realizados na ambiência do *software Oasis Montaj* 9.10 da *Geosoft*®. Na plataforma de Sistema de Informações Geográficas (SIG) do ArcGis 10.7.1®, foi integrados os dados multifontes. Esta integração deu suporte para extração de informação das litologias locais e identificação de quatro unidades litológicas: Sienito Itiúba, Unidade Santa Luz, Unidade São Bento e Complexo

do Vale do Jacurici. Nesta última unidade, foi aplicada a uma análise combinada entre Álgebra de Mapas e lógica *Fuzzy* entre todos os dados rasters de entrada, afim de balizar um zoneamento das áreas potenciais para ocorrência de rochas máficas-ultramáficas. Ao fim, notou-se uma boa relação entre os resultados e modelos geológicos de superfície presentes em bibliografias. Diante disto, a aplicação da metodologia utilizada trouxe uma análise integrada de dados multifontes para elaboração de um mapa de geologia das rochas máficas-ultramáficas e suas encaixantes do segmento Ipueira-Medrado no estado da Bahia.

Palavras-Chaves: Geoprocessamento; Vale do Jacurici; Cromita

1 Introduction

With the evolution of the metallurgical sector during the 20th century, chromite and other minerals became essential commodities, and its greatest and most common use is in producing stainless steel. In this context, the Vale Jacurici complex in Bahia has the largest chromite reserves in the world (Figueiredo 1977). Thus, with the continuous use of chromium by the foundry industries, the need for knowledge and exploration of new prospective targets to supply the market expanding needs.

Regarding the chromitiferous bodies of Vale do Jacurici, several studies have been conducted using aerogeophysical methods and digital image processing. Among these works, we can highlight Peixoto (2016), who employed magnetic and radiometric methods to identify mafic-ultramafic bodies in the northern portion of the São Francisco Craton, and Rebouças et al. (2023), who used digital satellite image processing methods for the zoning of chromitiferous bodies in Vale do Jacurici.

Due to its broad applicability, whether industrial, environmental, or even social, geoscientists have produced research based on the resolution of socio-environmental and economic dilemmas, supporting the advancement of geotechnologies. According to Bitar, Iyomasa and Jr. Cabral (2000), geotechnologies are connected to the need to characterize, evaluate and solve problems arising from the continuous relationship between human activities and the physical environment. Thus, linked to this basic premise, geotechnologies allow multisource data integration to interpret geomorphological and geological features. To this end, the use of remote sensors to characterize study targets is becoming more frequent.

Therefore, the present work aims to use Remote Sensing and aerogeophysical data to elaborate the geological map of the study area and highlight new areas for chromium prospection, and in this way to support studies already carried out and help to develop new ventures in mineral exploration.

2 Regional Geology

The São Francisco Craton (CSF) is located in the eastern portion of the South American platform and regionally outcrops in the Brazilian states of Bahia, Sergipe, and Minas Gerais. This is delimited to the south and west by the Brasília belt, to the northwest by the Rio Preto belt, to the north by the Riacho do Pontal and Sergipana belts, and to the southeast by the Araçuaí belt (Almeida 1977).

The study area is mainly inserted in crystalline terrains composed of deformed, folded, faulted, and metamorphosed mafic-ultramafic bodies, preferably oriented in the N-S direction in the Jacurici Valley Unit (Pilla Dias et al. 2021). The aforementioned unit is characterized by the geological domain of komatiitic, tholeiitic suites, and Banded Iron Formations (BIFs).

In the study area, the main lithotypes are metagabbronorites, chromitites, metapyroxenites, and methanorites intensely folded and fractured. These lithotypes are intrusive in the Santa Luz Complex, dated from the Mesoarchean, belonging to the Serrinha Block, which is subdivided into two units. The first unit corresponds to banded gneisses characterized by the alternation of gray gneiss rocks (with biotite, hornblende, microcline, plagioclase, and quartz, as main minerals) and amphibolitic bands with or without garnet. The second unit is composed of granodioritic to tonalitic orthogneisses with migmatitic structures (Carvalho & Ramos 2010).

To the west of the study area, the presence of the syenitic body (Syenite Itiúba) with gneissified edges is registered, and the central region has interaction between magmatic and metamorphic foliation, being part of the domain of intrusive and extrusive alkaline complexes. This lithology is also characterized by composing the sub-alkaline series (monzonites, fourth-monzonites, mangerites; Souza, Melo & Kosin 2002).

3 Material and Methods

3.1 Study Area

The study area is located in the municipality of Andorinhas, in the geographic region of Piemonte Norte do Itapicuru, in the central-north region of Bahia State. This municipality borders the municipalities of Senhor do Bonfim, Monte Santo, Jaguarari, Itibira, and Uauá and is located 450 km from Salvador, BA. The mafic-ultramafic complex of Vale do Jacurici is highlighted in Figure 1.
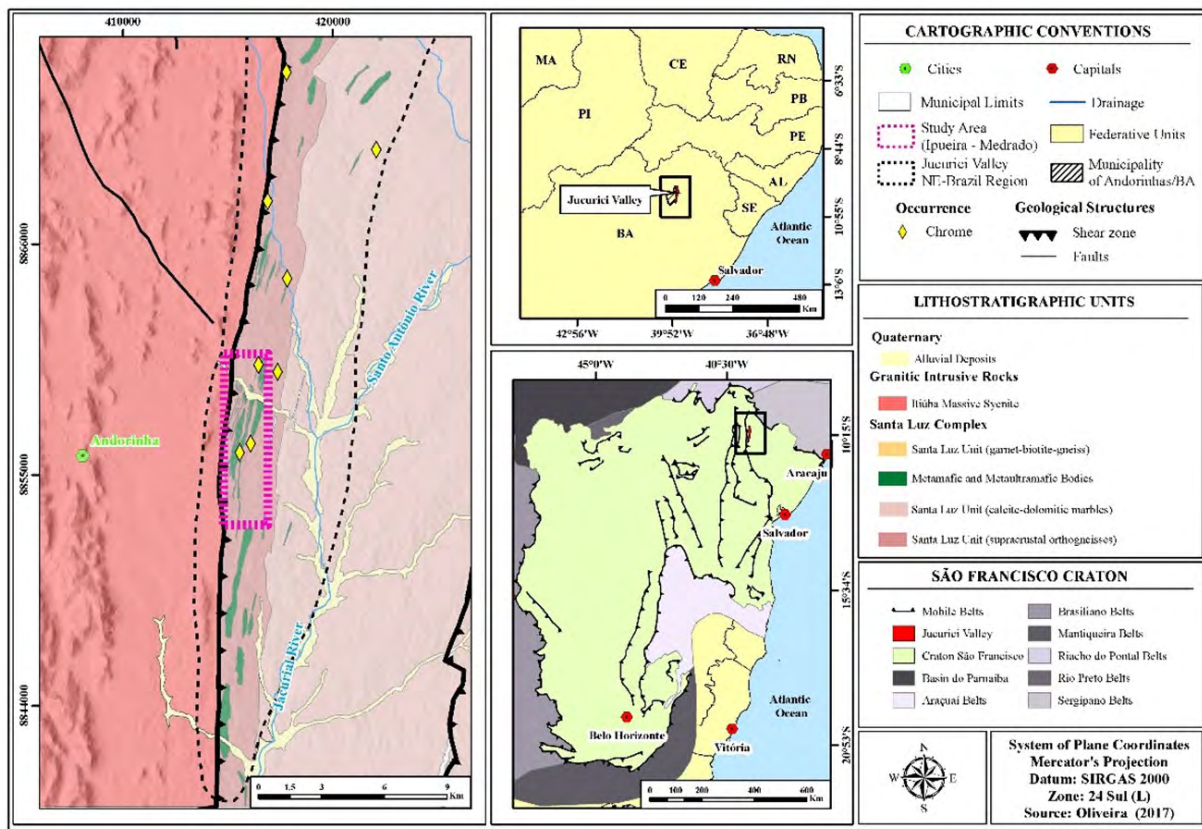
Figure 1 Location map of the study area and lithostratigraphy of a portion of the Jacurici Valley, emphasizing the region of the Ipueira-Medrado study area (Oliveira et al. 2016).

3.2 Satellite Images

This work uses optical images from the ASTER sensor aboard the Earth Observing System (EOS) TERRA and the RADAR image from the Alos satellite Palsar sensor. The platform on which the ASTER sensor is coupled travels in an almost circular orbit, synchronous with the Sun, with an inclination of 98.2° at an altitude of 705 km with image acquisition cycles every 16 days. This sensor (ASTER level 1B) has 14 bands. Two scenes were used to study the area in question: ASTB011005130520 and ASTB011005130529, obtained on October 5, 2001. Both can be accessed through the United States Geological Survey (USGS) website. The RADAR image from the Palsar sensor was acquired from the Alaska Satellite Facility (ASF) website and had a spatial resolution of 12.5m.

3.3 Aerogeophysical Data

The data used were provided by Companhia Baiana de Pesquisa Mineral – CBRM, referring to the aerogeophysical survey project of the Riacho Seco-Andorinha sector (code 3035). For the flight lines, transects were performed every 250m (east-west) and control lines every 2,500m (north-south). With a system attached to the aircraft with gammaspectrometry and magnetometry sensors, samples were collected every 0.1 and 1.0 s (magnetic and gammaspectrometry, respectively), with a Cs vapor sensor and 0.001 nT resolution (magnetic) and 256 spectral channels (gammaspectrometry) according to data from LASA (2002). Data acquisition was carried out between September 29, 2001, and December 26, 2001, by the company LASA Engenharia e Prospecções S/A.

3.4 Methods

3.4.1. Digital Image Processing

The RADAR image from the Palsar sensor was used for the morphological analysis of the study area through a Digital Terrain Model (DTM). For this purpose, a technique was implemented to enhance drainage features, roughness patterns, and terrain structures. The Hillshade algorithm in the ArcGis 10.7.1® software allows the implementation

of artificial light with delimited angles to highlight these features. The focus of the light applied to the Digital Terrain Model was positioned at an azimuth of 110° with a dip angle of 15°.

The optical images used were obtained initially in terms of radiance. Thus, radiometric correction using the Fast Line-of-sight Atmospheric Analysis of Hypercubes (FLAASH) algorithm (Kaufman et al. 1997) was necessary for the VIR and SWIR channel bands. This correction uses the infrared and shortwave wavelengths (<3μm) to correct images within the visible spectrum. It can be used for hyperspectral and multispectral sensors (Kaufman et al. 1997). Thermal bands were not used in the study.

Then, a mosaic of the scenes was created in the ENVI® 5.3 software to carry out the image processing. Among the processes, two techniques were employed: Principal Component Analysis (PCA) (Crosta 1992). Linear filters, histogram adjustments, and false RGB color compositions were also applied. In work in question, the PCA techniques were applied only to the VNIR and SWIR data.

3.4.2. Principal Component Analysis (PCA)

Principal Components Analysis (PCA) is a technique that allows us to determine the extent of the correlation between the bands and, through the appropriate mathematical transformation, to remove it. This correlation, in other words, is configured as a redundancy of information between the bands and is generated when there are many targets in the scene, such as vegetation or topographic shading. The PCA works precisely to eliminate the high correlation, segregating the noise in different layers with equal amounts to the input data (Meneses & Almeida 2012).

In the first three components generated, 99% of the spectral information of the bands is retained. In the other low-order PCAs, 1% of the information is also present with low signal-to-noise ratios. However, to enhance the information on some targets, it is interesting to combine high and low-order data (Amer, Kusky & Ghulam 2010).

Through this method, in summary, it is possible to verify the level of correlation between the bands and the degree of information or variance present in the data (Meneses & Almeida 2012).

This treatment is appropriate for sensor images with high numbers of spectral bands (Crosta 1992). The contrasts generated through the compartmentalization of information in this process increase spectral differences and mapping of lithological units (Liu et al. 2014). Thus, it is evidenced that features previously presented discreetly to the eyes.

3.4.3. Processing of Aerogeophysical Data

This entire research phase was carried out in the software Oasis Montaj 9.10 by Geosoft® and was divided into two stages. The first was known by data processing, and the second by interpreting radiometric and magnetic data with local geological information (Oliveira et al. 2016). The method is based on a compilation of aerogammaspectrometric and aeromagnetometric data processing (Peixoto 2016; Pilla Dias et al. 2021).

Among the products generated and applied to the research in question, in the field of radiometric data, were: normalized uranium (eU), normalized thorium (eTh), potassium (K), and the RGB ternary composition (eU, eTh, and K). Among the magnetic products, the derivative tilt of the magnetic field (Tilt Derivate) (Verduzco et al. 2004), Analytical Signal Amplitude (ASA) (Li 2006), Total Horizontal Gradient Amplitude (THGA) (Cooper & Cowan 2008), 1st Derivative of the Total Magnetic Field (Peixoto 2016).

3.4.4. Product Integration

Data integration was developed in the GIS environment of ArcGIS 10.7.1®. The input data in this procedure were the products of the previous processes: raster of the products of the orbital data of the magnetic and radiometric domains. For this, the input data were reclassified into low, medium, and high (Table 1). These classes were determined through the characteristic of the data and their responses to the occurrence of mafic-ultramafic rocks. For this, the radiometric responses were classified into high, medium and low values for the three channels of the radioelements Th, K and U.

Table 1 Reclassification of raster data for the composition of the Map of Occurrence Possibility of Mafic-Ultramafic Rocks.

Class/Product	Remote Sensing Products	Magnetic Domains	Radiometric Domains
Low	Itiúba Syenite	low and medium	1
Medium	Santa Luz and São Bento Unit	High	2
High	Vale Jacurici Unit	Very high	3 e 4

Source: Own elaboration.

With the new classes defined, a Map Algebra was carried out through the overlapping of the data to obtain a new raster developed by integrating the data. Then, through Fuzzy Logic, five classes were established for this raster in relation to the possibility of the occurrence of mafic-ultramafic rocks: "Very High," "High," "Medium," "Low," and "Very Low."

Among the approaches inherent to logic, there is the Fuzzy logic, which deals with uncertainty and imprecision, allowing variables and propositions to have values that vary between 0 and 1, unlike binary logics that vary only between true or false propositions. Thus, Fuzzy logic brings statements that can be partially true or partially false, reflecting the reality where many concepts are not absolute, but have gradations. In geosciences, fuzzy logic plays a fundamental role in supporting the manipulation of complex data and uncertainties, in stages of modeling, evaluation, optimization and decision-making regarding geological and geospatial data (Pereira et al. 2021).

In the end, a joint analysis of the aerogeophysical products and image processing with geology was used to extract information from the lithotypes. The analysis of the results was based on geological data from CPRM in the Andorinhas geological map (SC.24-Y-B-II) (Oliveira et al. 2016) and lithological-structural data from Almeida, Cabral and Bezerra (2017).

4 Results

4.1 Morphological Analysis (Radar)

The DTM obtained through processing the local radar image after implementing the artificial light technique was adopted as the basis for extracting information from the local structural features. According to Figure 2, it is possible to zone the study area into three large units. Through this model, three features with different relief patterns are noted on the terrain. The western portion of the model presents a less irregular pattern, with more significant accidents on the ground. In the center-east segment of the model, two features can be seen: rough features with preferential lineaments (center), less rough features with diffuse lineaments, and a higher topographic level than the central portion (east).
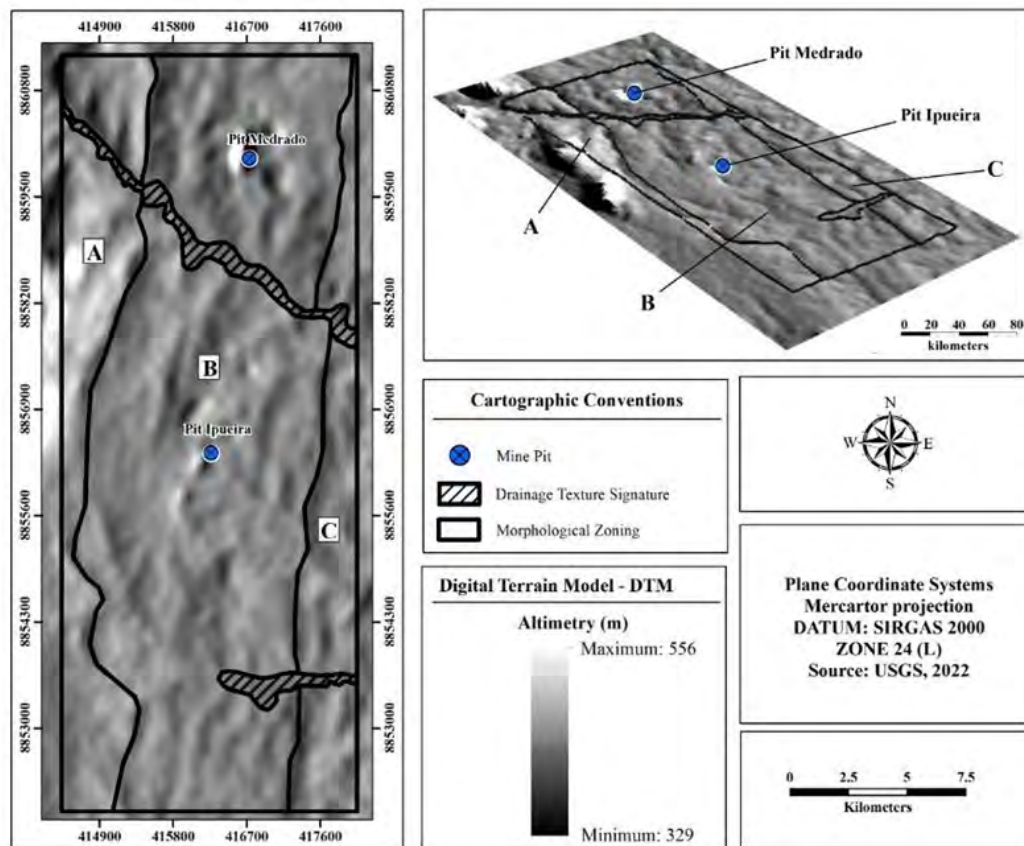

Figure 2 Delimitation of zones of textural signatures of the terrain extracted through the Radar image of the Alos satellite Palsar sensor with artificial light in the azimuth of 110° and 15° of incidence.

Through the observed textural patterns, "A," "B," and "C" were interpreted as lithological units. Unit "A" presents a textual signature marked by a portion with topographic elevations. The southernmost part of unit "A" is flat, not very rough, and without apparent structural controls. Unit "B," on the other hand, presents a different pattern from the aforementioned one, where the terrain is rougher, with well-marked structural controls and oriented in the N-S direction. Unit "C," like "B," also presents apparent structural controls but is less expressive and has a diffuse orientation than the others. In Figure 2, some drainage patterns can also be observed.

4.2 Principal Components Analysis (Optical Images)

The PCA was applied to all nine bands of the Aster sensor (VIR-SWIR). When analyzing the generated statistical matrices of correlation and covariance, it was noticed that there is a positive correlation between the bands. However, for the covariance, the values are close to zero, which highlights the independence between them. The first component (PCA1) represents 97.72% of the data variance. Among the first three main components of higher order (PCA1 to PCA3), 99.52% of the band information is retained.

Due to linear transformations performed by the processing, the eigenvectors were generated. Through a matrix composed of the eigenvectors (Table 2) together with the knowledge of the spectral response of the chromite within the ranges of the sensor worked, the following were chosen for the false color RGB composition of the main components: PCA6 (red), PCA9 (green) and PCA 1 (blue). The choice of these main components was based on the bands' greatest contributions to the compositions of the PCA.

A false-color RGB product was generated for lithological analysis using the selected PCAs. This product can be visualized in Figure 3, and its interpretations focus on the study area's central portion. Through the results obtained, zones aligned in the mostly N-S direction were vectorized in the central portion of the study area. These zones are presented in reddish brown tones (Figure 3A-B) and, according to the bibliography (Marinho et al. 1986; Almeida, Cabral & Bezerra 2017), is correlated to the mafic-ultramafic intrusive bodies of the Jacurici Valley. The dark blue portions outline the spectral responses of tailings piles and/or chrome mine yards.

With this method, there was a minor enhancement of the enclosing lithotypes and structural control of the area, thus making unfeasible the delineation of syenogranite, granulite, and the orthogranulite that are described in the literature. Thus, the PCA RGB results were applied only to enhance the bodies of the Complex Jacurici Valley.

4.3 Magnetic Results

Given the results of magnetic data processing, the limits of edges and anomalous centers of some geological bodies were extracted. In a joint analysis, through the ASA (Figure 4A) product and the first derivative of the magnetic field, the extraction of the limits was allowed, and the zoning of the anomalous bodies was carried out, as shown in Figure 5.

The result of the ASA product did not show clear delimitations in the lower portion of the area. The lowest values of this product (<0.3nT/m) are diffuse. However, higher values in the order of 0.8 nT/m are visualized in the most central portion and aligned in the N-S direction.

Table 2 Contribution of the Bands to the creation of the PCA.

| Eigen-vectors	B1	B2	B3	B4	B5	B6	B7	B8	B9
PCA1	-0.33	-0.33	-0.33	-0.34	-0.34	-0.34	-0.33	-0.33	-0.34
PCA2	0.54	0.46	0.37	-0.21	-0.14	-0.07	-0.35	-0.31	-0.28
PCA3	-0.26	-0.45	0.79	0.22	0.04	0.01	-0.12	-0.20	-0.01
PCA4	0.10	-0.03	0.28	-0.23	-0.48	-0.53	0.47	0.34	0.09
PCA5	-0.18	0.00	0.15	-0.55	0.08	0.51	0.40	0.05	-0.46
PCA6	-0.08	0.19	-0.08	0.55	0.06	-0.24	0.44	-0.27	-0.57
PCA7	-0.69	0.64	0.15	0.04	-0.18	0.00	-0.19	0.15	0.08
PCA8	0.03	0.01	-0.07	0.16	-0.64	0.44	0.23	-0.46	0.30
PCA9	0.13	-0.16	-0.03	0.33	-0.42	0.29	-0.30	0.57	-0.41

Source: Own elaboration.
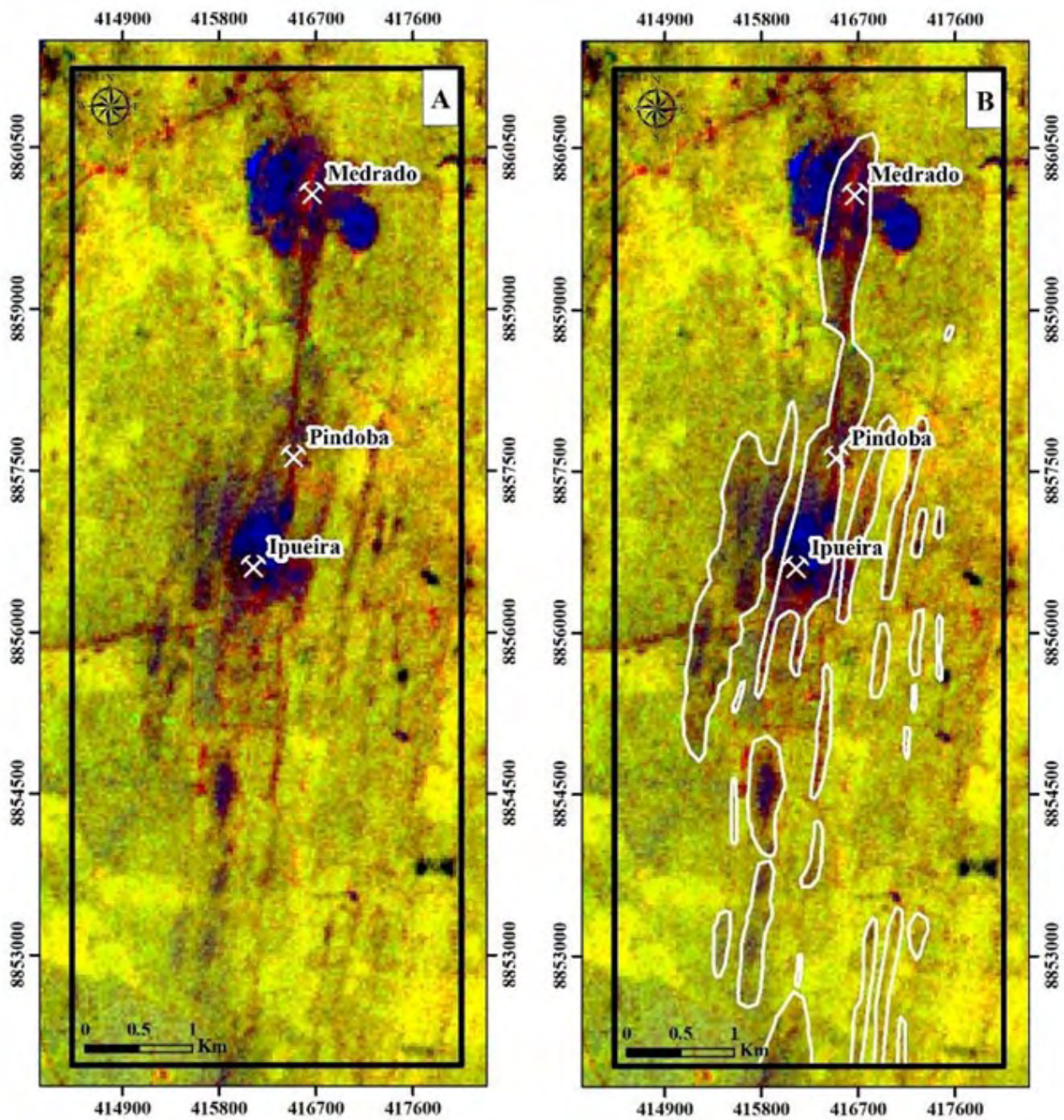
Figure 3 PCA products: A. RGB false colors of the PCA; B. N-S aligned zones in continuous white lines.

Through the first derivative on the x-axis, the boundaries of the lithotypes were visible between contrasts of high (>0.4nT/m) and low (>-0.1nT/m) magnetic values (Figure 4B). A very sharp contrast between the magnetic peaks is observed along the entire left portion of the area. In the central portion, this contrast is again similar to the previous one, forming a non-continuous magnetic anomalous zone with well-marked contrasts between maximum and minimum values (-0.5 and 0.4nT/m, respectively). To the east, concentrated from the upper to lower portion of the area under analysis, two boundary patterns are visualized. The first contrast is observed in the northern portion between -0.5nT/m and 0.4nT/m, and the second, with less contrast in the southern portion between -1.0 and 0.2nT/m.
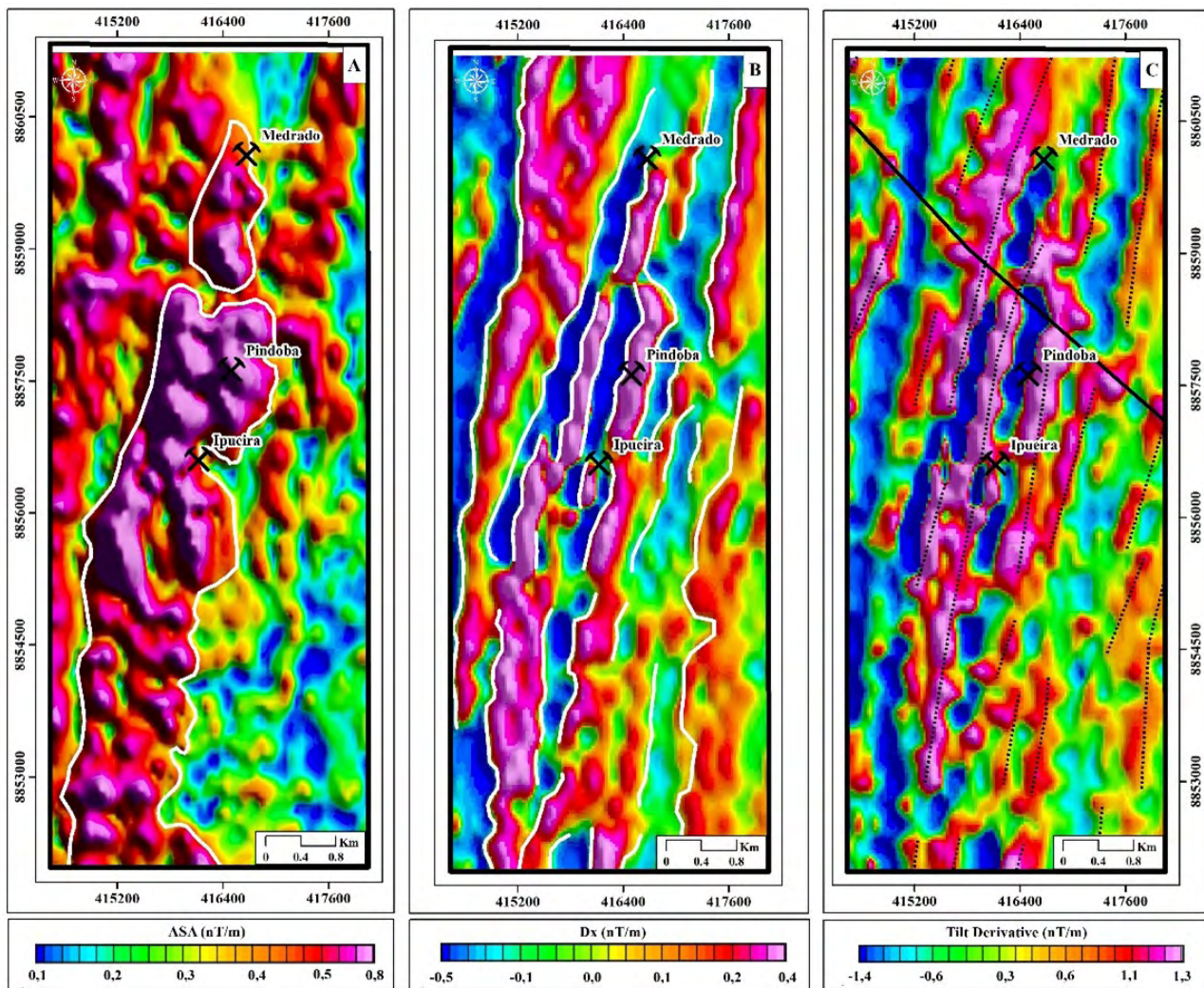
Figure 4 Magnetic Products: A. ASA product, with anomalous central body outlined in a white line; B. Product of the first horizontal derivative on the x-axis highlighting the western and eastern edges of the area, and a portion with an anomalous zone in the central portion. All products feature shading at 45°; C. Tilt Derivative product.

Results were also obtained for two other filters to identify anomalous edges and bodies: the first vertical derivative and the Tilt Derivative (Figure 4C). This product also highlights limits better represented by the first horizontal derivative and ASA, allowing the transmission of magnetic lineaments oriented in the NNE-SSW direction.

A final map was created for general analysis by crossing the information from the identified magnetic domains with the magnetic lineaments (Figure 5). In this map, the classification of magnetic domains into three classes was discussed: low (<0.1 nT/m), medium (0.2 to 0.3 nT/m), and high (>0.3 nT/m) magnetism.

4.4 Radiometric Results

Eight radiometric products were generated: (1) eTh, (2) eU, (3) K, (4) RGB (K, eTh, and eU). For the eTh, eU, and K channels, the following classes were created: "high," "medium," and "low" content (Table 3) by analyzing the histograms.

Through the results of the radiometric data, responses were obtained for the K, eU, and eTh channels. In Figure 6A, potassium anomalies (>5.6%) are visualized across the western edge of the study area. A potassic anomaly can also be visualized diagonally, crossing the northernmost

portion. However, in the rest of the area, concentrations in medium and low orders are noted in terms of radiances <1.7%. The primary anomalies (>0.63ppm) are concentrated on the west edge of the upper portion of the study area and other smaller ones in the south and center-south.

In Figure 6B, the distribution of thorium is observed in directions aligned with the directions described in the bibliography (N-S). Values greater than 0.6 ppm are found in almost all areas. However, a soft radiance is noted across

the eastern border and at some points in the center of the map (< 6.1 ppm). In the eTh and K channels, a well-marked structure is observed diagonally in the northern portion of the area. In this structure, anomalies are observed in high values for potassium and thorium and an anomaly in smaller proportions for uranium. In the eU channel data, however, a positive anomaly is seen across the western border and further south of the study area (Figure 6C).
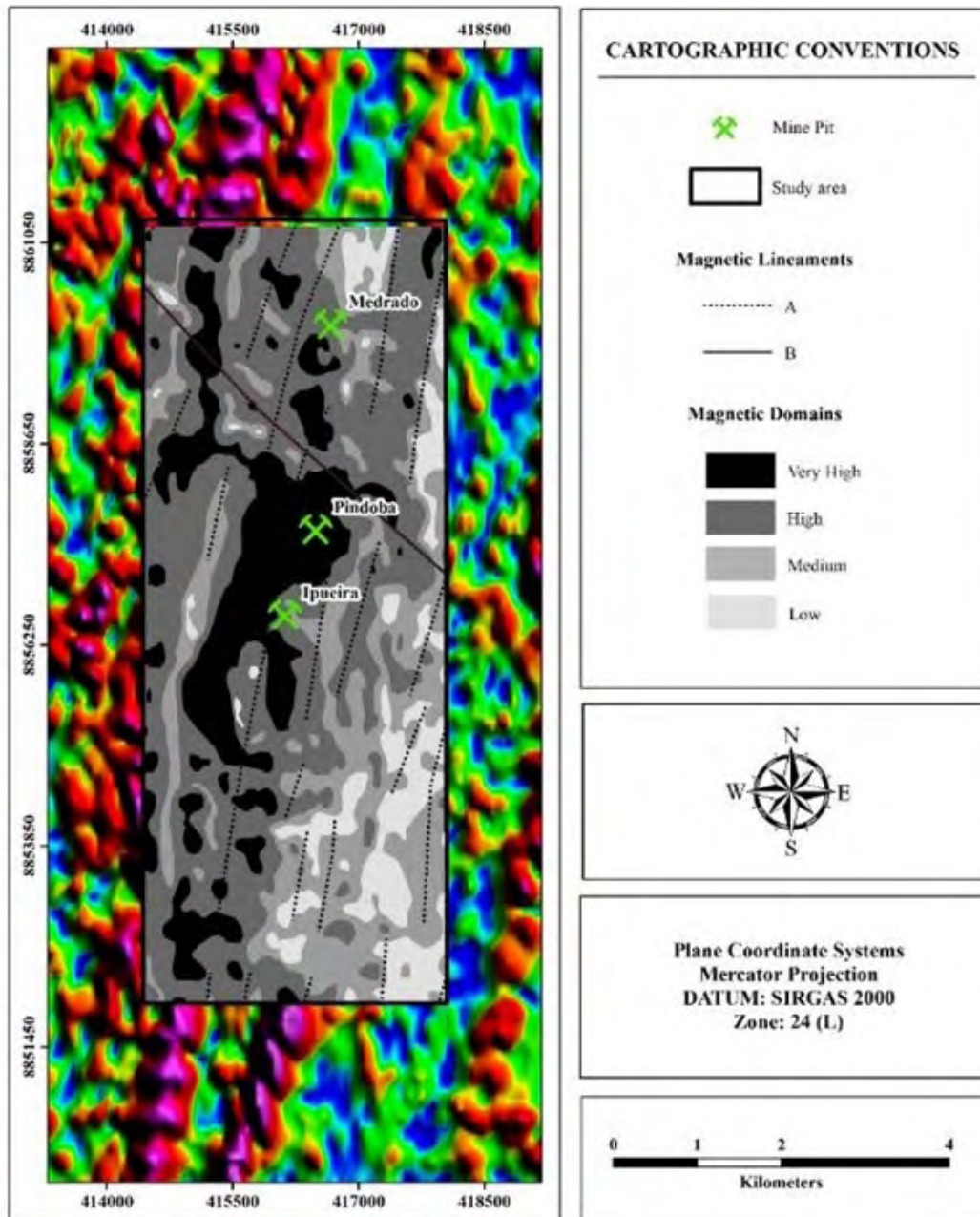

Figure 5 Magnetic Domains using Analytical Signal Amplitude with Magnetic Lineaments extracted from the first vertical derivative and Tilt Derivative.

Table 3 Radiometric classes.

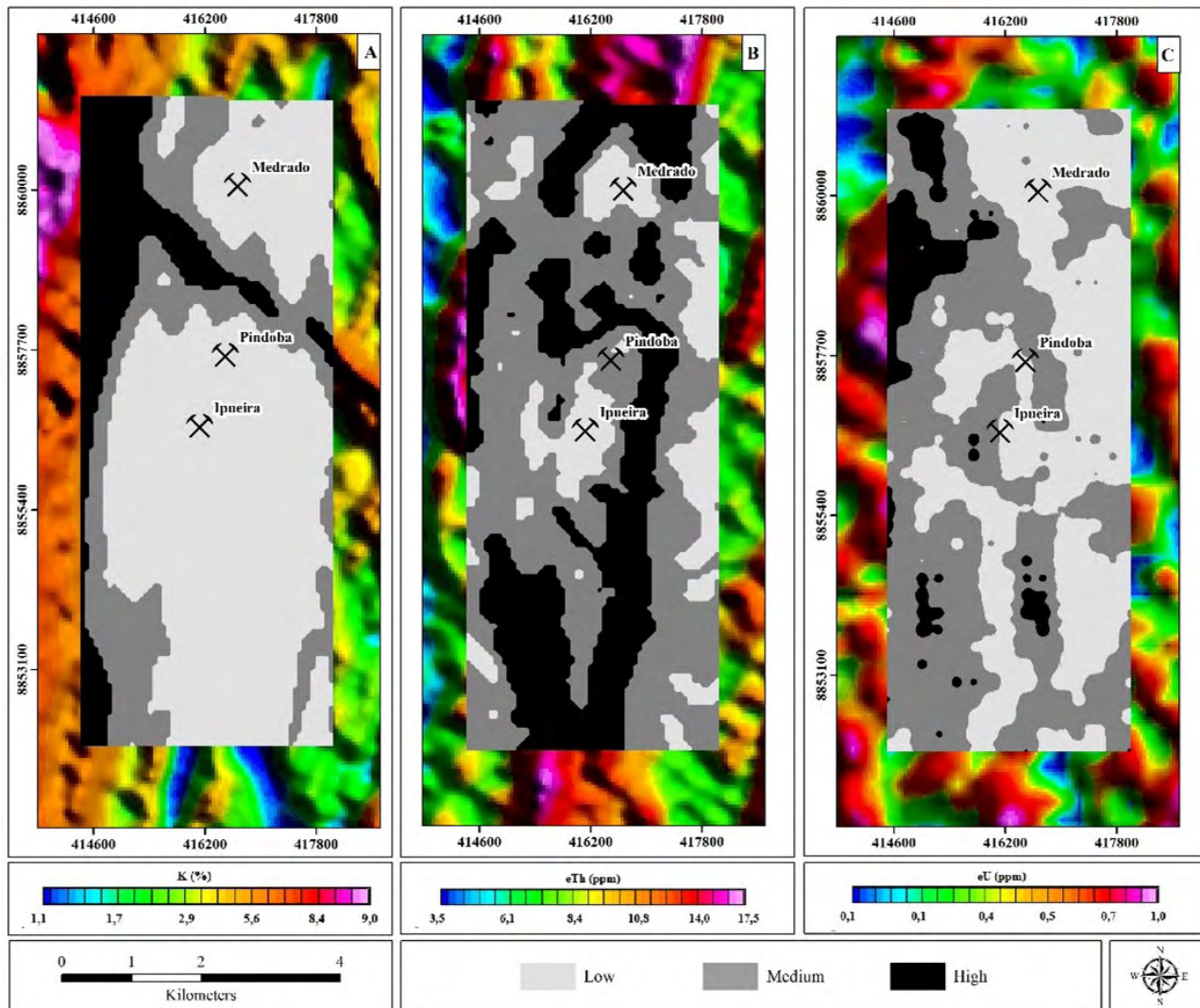|	K (%)	eTh (ppm)	eU (ppm)
Low	<2.38	<7.91	<0.31
Medium	2.38 to 4.12	7.91 to 10.91	0.31 to 0.63
High	>4.12	>10.91	>0.63

Source: Own elaboration.

Figure 6 Interpretations of radioelements: A. K; B. Th; C. U.
Source: Own elaboration.

A final map crossed this classification information through the interpretations of the three channels (K, U, and Th) and subdivisions into high, medium, and low classes. The map generated through the map algebra technique generated zones with varying significance levels for each radioelement.

The ternary map allows the zoning of anomalies of two or three radioelements. Using the ternary, the area was divided into gamma-spectrometric domains: "1", "2", "3," and "4" (Figure 7). The highlights are observed since the RGB composition highlights parts with a high element count, with the maximum concentrations of the

three channels in white and the minimum in black. In RGB ternary false color rendering, the following elements were assigned to each channel, respectively: R (K), G (Th), and B (U).

The first established domain, "1," presents very high values for the radioelement K and low values for U and Th. This domain is marked with red channel colors, which shows the large amount of K. Linked to this domain, a SE-NW structure is observed crossing the area in the northern portion. Domain "2" has high Th contents, moderate U contents, and low K contents.

Radiometric domain "3" presents darker colors, which may be associated with low concentrations of the three radioelements. Due to its coloration in the RGB composition, this domain can also be associated with mafic-ultramafic rocks and marbles. In the central portion of this domain, a slight U anomaly is visualized and was named domain "4".
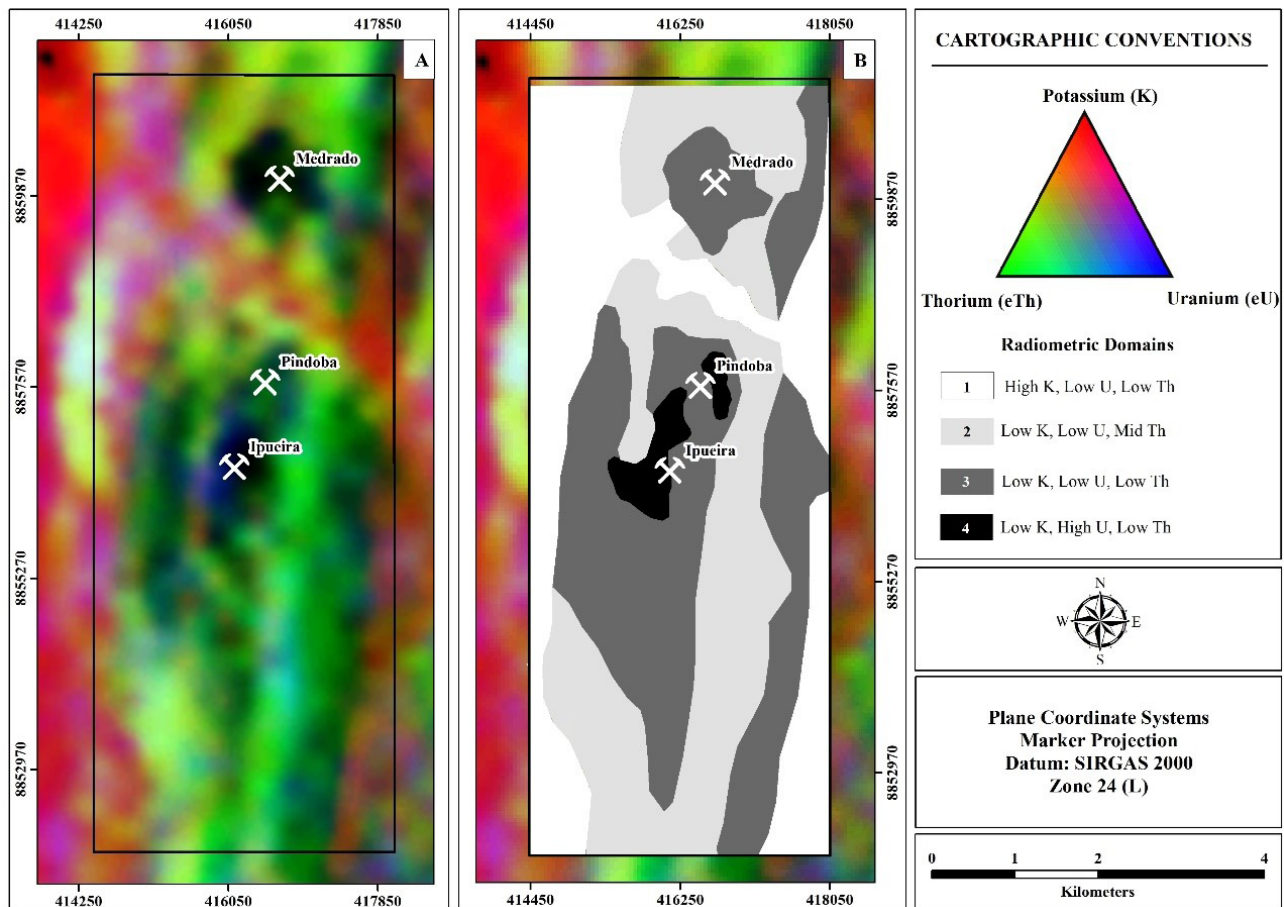

Figure 7 Ternary composition of radiometric data: A. Ternary RGB Composition; B. Radiometric Domain Interpretations (Red: potassium; Green: thorium; Blue: uranium).

4.5 Final Geological Map

All the processing results were incorporated into the composition of the final map (Figure 8). Thus, with the integrated results, lithological limits were adjusted through magnetic anomalies and analysis of radiometric channels, as well as through the targets' spectral responses and textural signatures.

When analyzing the results of the mafic-ultramafic rocks, the targets that presented some correlation with the bibliographic records were kept in the final map. The other targets were demarcated as targets that have an appropriate level of importance for mineral research, as shown in Figure 8. Structural controls observed in studies at regional and local levels registered in the bibliography were also added to the map, which was similar to the answers

obtained through the processing in the present work. Among these structures, the fault is embedded in the study area in the NW-SE direction in the upper portion of the map, and the shear zone is present on the right edge of the Itiúba syenite. This zone is part of the set of shear zones on the west edge of the Serrinha block.
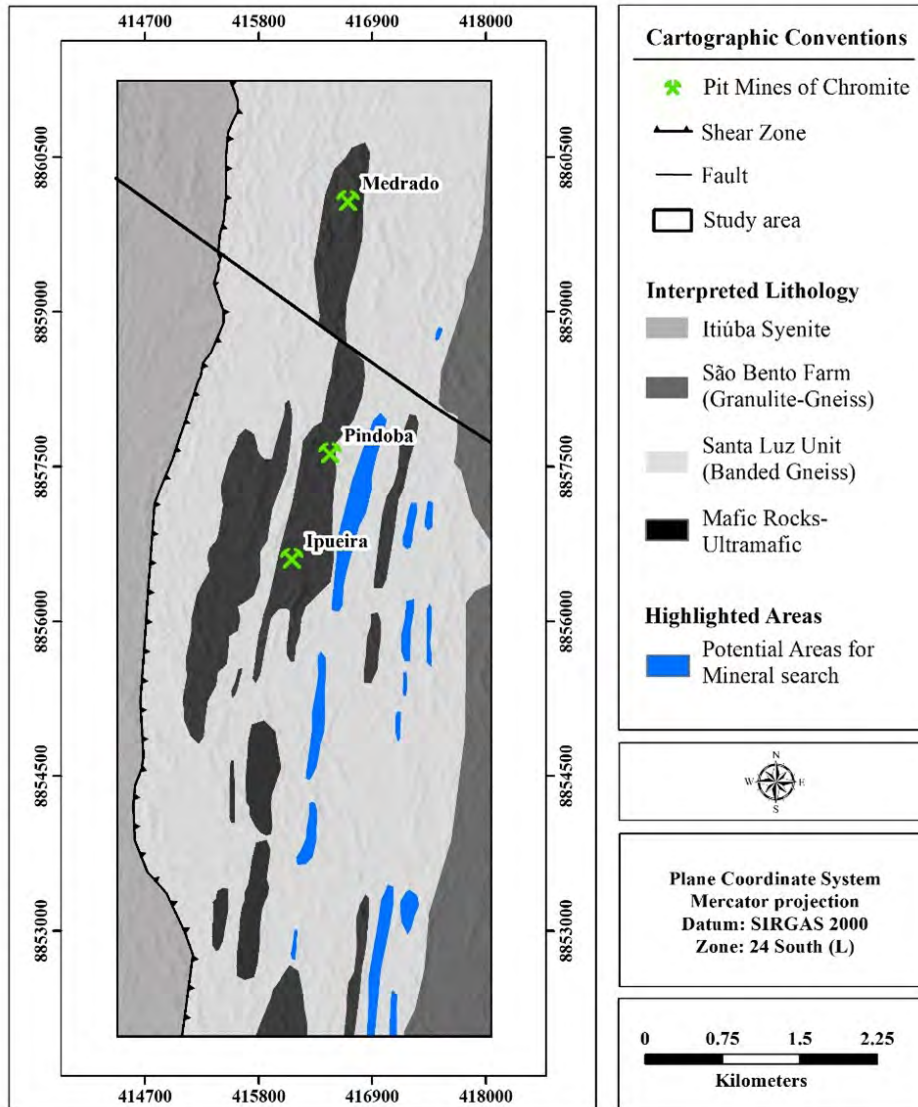

Figure 8 Final Geological Map produced in this work.

5 Discussions

5.1 Itiúba Syenite

The Itiúba syenite (unit "A") presented a textural signature feature typical of granitoids, with a slightly rough relief, and topographically it appears as a higher terrain than the adjacent ones. This difference in roughness and morphological characteristics stands out compared to the units composed of granulites and granulites-gneiss. As it is a syenogranite, it presents a low magnetic response. However, as it is located east of a shear zone, the border made between the syenite and the gneiss granulites presents a magnetic anomaly along this zone. This anomaly may be related to zones of mineral alteration and enrichment of ferromagnetic materials. Its high values are present in the K channel, and low eTh and eU values are typical of ultrapotassic syenitic rocks.

Linked to the syenitic body, a structure is seen cutting the study area in the NW-SE direction. In this structure, the drainage is embedded geomorphologically, and along it, a strong potassic anomaly is noticed. Thus, this structure is similar to a possible pegmatitic vein originating from syenite.

5.2 Santa Luz Unit

Thrust structures from the east strongly mark the Santa Luz unit to the west (morphological unit "B"). With this orientation, structures oriented in the N-S direction were formed, where according to the bibliography, their features are similar to the granulitic gneisses of the Santa Luz Unit. Other lithologies are also present in this unit, such as metagabbronorites, chromitite, metapyroxenite, methanorite, and marble lenses. Thus, with this lithological configuration, a low to medium magnetic response is seen, and low radiometric values for K and eU and high for eTh. These magnetic responses are typical of the rocks in this unit and contrast firmly with the mafic-ultramafic rocks of the Jacurici Valley complex.

5.3 Fazenda São Bento Unit

Unlike the other units described, the granulites from the Fazenda São Bento Unit (morphological unit "C") present a textural signature that is less prominent. However, as it is a more distal portion of the shear zone between the Itiúba Syenite and the rocks of the Santa Luz Unit, these granulites show little influence of the N-S oriented structural control. What is observed are orientation patterns between diffuse and slightly NE-SW oriented. This ends up generating a rougher morphology. In general, it presented a low magnetic response. However, through some magnetic anomalies identified through the first horizontal derivative, the limits of the east edge of the São Bento Unit were delineated. Their magnetic responses are similar to the Santa Luz Unit, with K channel values between medium to high and low and medium for eU and eTh.

5.4 Mafic-Ultramafic Rocks of the Jacurici Valley Complex

The rocks of the mafic-ultramafic complex of Jacurici Valley, among the aforementioned units, were the only ones for analysis that obtained good results through the PCA method. With this method, an orientation of the well-marked bodies in the N-S direction was recorded. However, it was impossible to subdivide lithotypes that presented similar spectral responses when applying this method. These lithologies contain regular deposits of Banded Iron Formations (BIF) and mafic granulites that cannot be distinguished from chromitites and serpentinites using this method. The zoning of the mafic-ultramafic portion is well highlighted through the responses of magnetic methods, where products such as ASA and AGHT circumvented the anomaly boundaries well. These types of rocks generally present low values for the three radioelements. Within these zones, minor eU anomalies are observed. These anomalies may be related to hydrothermal changes or are linked to host metamorphic rocks of the Santa Luz Unit.

This condition makes sense since the granite has a low magnetic response and high radiance in the K channel. In contrast, the units in the Jacurici Valley were also well marked in the "Very High" class on the same map. This is due to the low radiance response of the three radioelements and the high magnetic response. These areas also showed correlations with already mapped areas with the occurrence of mafic-ultramafic rocks (Oliveira et al. 2016; Almeida, Cabral & Bezerra 2017).

6 Conclusion

With this study, it was possible to implement different geoprocessing techniques for orbital images and treatments of magnetic and radiometric aerogeophysical data for geological characterization. Each technique used allowed obtaining specific information about the structural controls and dimensions of the limits of the lithological bodies. Using the radar data, the limits of the lithologies of the Santa Luz and Fazenda São Bento Units were structured, as well as the patterns of the textural signatures of the Sienito Itiúba. With the technique of Analysis of Principal Components, a good efficiency was found for the prevention of spectral responses, which, according to the bibliography, are concentrated in the mafic-ultramafic bodies of the Vale do Jacurici Complex. The airborne physical data complemented the delineation of magnetic anomalies and the lithological interpretation through the radiometric responses of the U, Th and K channels.

The Itiúba Syenite and the mafic-ultramafic rocks of the area were the lithologies that presented the most expressive responses through the employed methods. The mafic-ultramafic bodies follow the pattern observed in the bibliography. This pattern is observed through alignment in the N-S direction and is mainly embedded in granulites from the Santa Luz unit. It was also noted that a strong potassium enrichment followed the NW-SE structure, where the local drainage was inserted. This potassium anomaly may be genetically correlated to the syenite, raising the hypothesis of a possible pegmatite. However, field studies and testimonies analysis of drillings in this segment are necessary for such a statement.

When comparing the results with the bibliography used as a basis for the research, the mafic-ultramafic bodies obtained in the work that presented correlation with the base material, were highlighted as mafic-ultramafic rocks. The other bodies were highlighted as potential areas for mineral research, as shown in the Final Map. However, the Principal Component Analysis (PCA) method presented difficulty in differentiating the rocks from the Vale Jacurici complex, the BIF, and the mafic granulites due to the similarity in the spectrometric responses. In the end, the methodology used for geological characterization presented satisfactory results that can be used for elaborating materials for field activities. Furthermore, these results identified new targets as potential areas for mineral research.

7 References

Almeida, F.F.M. de. 1977, 'O Cráton de São Francisco', *Revista Brasileira de Geociências*, vol. 7, no. 4, pp. 349-64, DOI:10.25249/0375-7536.1977349364.

Almeida, H.L., Cabral, E.B. & Bezerra, F.X. 2017, 'Evolução deformacional das rochas do Vale do Jacurici: implicações para a estruturação dos corpos cromitíferos máfico-ultramáficos', *Revista do Instituto de Geociências*, vol. 17, no. 2, pp. 71-88, DOI:10.11606/issn.2316-9095.v17-398.

Amer, R., Kusky, T.M. & Ghulam, A. 2010, 'New methods of processing ASTER data for lithological mapping: examples from Fawakhir, Central Eastern Desert of Egypt', *Journal of African Earth Sciences*, vol. 56, no. 2-3, pp. 75-82, DOI:10.1016/j.jafrearsci.2009.06.004.

ASF – Alaska Satellite Facility, *Distributed Active Archive Center*, viewed 15 November 2022, <https://search.asf.alaska.edu/#/>.

Bitar, O.Y., Iyomasa, W.S. & Jr. Cabral, M. 2000, 'Geotecnologia: tendências e desafios', *São Paulo em Perspectiva*, vol. 14, no. 3, pp. 78-90, DOI:10.1590/S0102-88392000000300013.

Carvalho, L.M. & Ramos, M.A.B. (orgs) 2010, *Geodiversidade do estado da Bahia*, CPRM, Salvador.

Cooper, G.R.J. & Cowan, D.R. 2008, 'Edge Enhancement of Potential-Field Data Using Normalized Statistics', *GEOPHYSICS*, vol. 73, no. 3, pp. 1MJ-Z46, DOI:10.1190/1.2837309.

Crosta, A.P. 1992, *Processamento digital de imagens para sensoriamento remoto*, Instituto de Geociências, UNICAMP, Campinas.

Figueiredo, A.N. 1977, 'Depósitos de cromita em Goiás e Campo Formoso (BA) – diagnóstico e análise comparativa', Revista Brasileira de Geologia, vol. 7, no. 1, pp. 73-83.

Kaufman, Y.J., Wald, A.E., Remer, L.A., Gao, B.-C., Li, R.-R. & Flynn, L. 1997, 'The MODIS 2.1-μm channel-correlation with visible reflectance for use in remote sensing of aerosol', *IEEE Transactions on Geoscience and Remote Sensing*, vol. 35, no. 5, pp. 1286-98, DOI:10.1109/36.628795.

LASA Prospecções 2002, *Projeto de Levantamento Aerogeofísico da Área Riacho Seco – Andorinha*, Relatório Final, SICM/CBPM, Rio de Janeiro.

Li, X. 2006, 'Understanding 3D analytic signal amplitude', *GEOPHYSICS*, vol. 71, no. 2, pp. 1MA-Z34, DOI:10.1190/1.2184367.

Liu, L., Zhou, J., Yin, F., Feng, M. & Zhang, B. 2014, 'The reconnaissance of mineral resources through ASTER data-based image processing, interpreting and ground inspection in the Jiafushaersu Area, West Junggar, China', *Journal of Earth Science*, vol. 25, no. 2, p. 397-406, DOI:10.1007/s12583-014-0423-9.

Marinho, M.M., Rocha, G.F., Deus, P.B. & Viana, J.S. 1986, 'Geologia e potencial cromítico do Vale do Jacurici-Bahia', apresentado no 34º Congresso Brasileiro de Geologia, pp. 2074-88.

Meneses, P.R. & Almeida, T. (orgs) 2012, *Introdução ao processamento de imagens de sensoriamento remoto*, Universidade de Brasília, CNPq, Brasília.

Oliveira, R.C.L.M., Neves, J.P., Pereira, L.H.M., Macêdo, L.L., Mota, E.L., Santiago, R.C. & Teixeira, L.R. 2016, *Folha SC.24-Y-B-II Andorinha: mapa geológico - escala 1:100.000*, CPRM, Salvador.

Peixoto, V.M. 2016, 'Caracterização geofísica da região do Complexo Cromitífero de Jacurici-BA com auxílio de Aeromagnetometria e Aerogammaespectrometria', TCC, Instituto de Geociências, Universidade Federal do Rio Grande do Sul, Porto Alegre.

Pereira, G.A., Campos, A.B., Silva, P.J. & Carvalho, D. 2021, 'Lógica fuzzy aplicada à criação de um mapa geotécnico de saída para a urbanização da área de expansão da UNICAMP-Campinas, SP', *Geociências*, vol. 40, no. 4, pp. 1137-45, DOI:10.5016/geociencias.v40i04.15478.

Pilla Dias, J.R., Bertolini, G., Charão Marques, J., Frantz, J.C., Sobrinho de Silveira, C.J. & Cezario, N. 2021, 'Análise prospectiva de corpos máfico-ultramáficos através da aerogeofísica: estudo de caso do vale do Jacurici/Bahia', *Revista Nordeste de Geociências*, vol. 7, no. 2, pp. 271-81, DOI:10.21680/2447-3359.2021v7n2ID23952.

Rebouças, I.S., Huhn, S.R.B., Miranda, M.P., Oliveira, P.H.B., Salgueiro, A.R.G.N.L. & Duarte, C.R. 2023, 'Processamento Digital de Imagens Aplicado à Caracterização Geológica: Depósito Máfico-Ultramáfico, Ipueira-Medrado, Bahia', apresentado em Anais do XX Simpósio Brasileiro de Sensoriamento Remoto, Florianópolis.

Souza, J.D., Melo, R.C. & Kosin, M. (coord) 2002, *Mapa geológico do estado da Bahia*, versão 1.1, CPRM, Salvador.

USGS – United States Geological Survey, *EarthExplorer*, viewed 3 November 2022, <https://earthexplorer.usgs.gov>.

Verduzco, B., Fairhead, D., Green, C.M. & MacKenzie, C. 2004, 'New Insights into Magnetic Derivatives for Structural Mapping', *The Leading Edge*, vol. 23, no. 2, pp. 116-9, DOI:10.1190/1.1651454.

Author contributions
Iago Silva Rebouças: conceptualization; formal analysis; methodology; validation; writing-original draft; writing – review and editing; visualization. **Sérgio Roberto Bacelar Hühn**: validation; writing – review and editing; supervision. **Mateus de Paula Miranda**: methodology. **Ana Rita Gonçalves Neves Lopes Salgueiro**: validation; writing – review and editing. **Kleiton Camilo da Paz Sales**: supervision; validation. **Cynthia Romariz Duarte**: validation; writing – review and editing.

Conflict of interest
The authors declare no conflict of interest.

Data availability statement
The data used in the work in question can be obtained through the United States Geological Survey (USGS; https://www.usgs.gov) and Alaska Satellite Facility (ASF; https://asf.alaska.edu) websites to acquire satellite image data. Data relating to geological modeling and surface geological data can be acquired through, respectively, FERBASA (https://www.ferbasa.com.br) and the Institutional Geoscience Repository (CPRM; https://rigeo.cprm.gov.br/handle/doc/16625).

Editor-in-chief
Dr. Claudine Dereczynski

Associate Editor
Dr. Gustavo Luiz Campos Pires